

# ‘Interaction annealing’ to determine effective quantized valence and orbital structure: an illustration with ferro-orbital order in WTe<sub>2</sub>

Ruoshi Jiang (姜若诗),<sup>1,2,\*</sup> Fangyuan Gu (顾方圆),<sup>1,\*</sup> and Wei Ku (顧威)<sup>1,2,3,4,†</sup>

<sup>1</sup>*Tsung-Dao Lee Institute, Shanghai Jiao Tong University, Shanghai 200240, China*

<sup>2</sup>*School of Physics and Astronomy, Shanghai Jiao Tong University, Shanghai 200240, China*

<sup>3</sup>*Key Laboratory of Artificial Structures and Quantum Control (Ministry of Education), Shanghai 200240, China*

<sup>4</sup>*Shanghai Branch, Hefei National Laboratory, Shanghai 201315, People’s Republic of China*

(Dated: July 4, 2024)

Strongly correlated materials are known to display qualitatively distinct emergent behaviors at low energy. Conveniently, the superposition principle of quantum mechanics ensures that, upon absorbing quantum fluctuation, these rich low-energy behaviors can *always* be effectively described by dressed particles with fully quantized charge, spin, and orbitals structure. Such a powerful and simple description is, however, difficult to access through density functional theory (DFT) calculations, since in terms of bare particles the quantum fluctuation would heavily smear the quantized quantities. To address this difficulty, we propose an ‘interaction annealing’ approach to decipher the dominant valence and orbital structure by suppressing the charge fluctuation through enhancing ionic charging energy. Applying this approach to ferroelectric semi-metal WTe<sub>2</sub> as a demonstration, we identify a dominant ferro-orbital ordered structure with W ion in a  $d^2$  spin-0 configuration. The proposed approach is straightforward to implement in standard DFT calculations to grant additional access to essential low-energy physics.

Modern functional materials [1, 2] display a rich variety of qualitatively distinct behaviors [3], sometimes even switchable under weak change of external conditions, such as temperature, pressure, strain, or external fields [4–7]. Generically speaking, such rich physical properties are almost always associated with the strong underlying many-body correlation in the electronic charge, orbital, spin, or lattice degrees of freedom [8]. Particularly, the ability to qualitatively switch the properties of these functional materials indicates the existence of multiple quasi-stable electronic structures with significantly different coupling strengths to various external conditions.

For complex systems like these, fortunately, there generally exist accurate effective descriptions capable of capturing the essential low-energy dynamics using only the most relevant *quantized* degrees of freedom. Such simplification originates from the superposition principle that leads to quantization of energy, particle number, orbital, and spin, and correspondingly a significant reduction of the number of low-energy relevant states. Consequently, the dynamics are mappable to those of a few dominant structures with quantized valence and orbital structure (accompanied by their quantum fluctuations). A good example is the great success of integer valence count in chemistry for example in determining stability of chemical compounds and solid materials [9–12].

However, such simple quantized effective descriptions are not easily accessible in the standard density functional theory (DFT) [13, 14] calculations. Indeed, due to the generic quantum fluctuation, the DFT results always contain non-quantized expectation value of valence, orbital and spin structure. This is because the above-mentioned effective quantized descriptions makes use of *dressed* particles that absorb all the rapid dynamics of higher energy, instead of the bare particles described by DFT. It is therefore highly desirable to seek a simple mean for direct access to such quantized effective description within the

current DFT framework.

Here, to address this important issue, we propose an ‘interaction annealing’ approach easily adaptable in standard DFT calculations. Using the two-site Hubbard model [15, 16] as a representative example, we first demonstrate the rigorous emergence [8] of such effective theories with *quantized* valance and orbital in different physical regimes. We then illustrate an adiabatic connection of the emergent structures in realistic regimes to the clean electronic structures with suppressed fluctuation, through boosting the dominant physics. Using the ferroelectric semi-metal WTe<sub>2</sub> as an example, we demonstrate the same generic adiabatic connection via DFT calculations. Based on this generic connection, we propose an ‘interaction annealing’ procedure to extract the quantized valance and orbital structure that dominates the low-energy dynamics. For the specific case of WTe<sub>2</sub> [17–30], this procedure identifies a dominant ferro-orbital ordered structure with W ions in a  $d^2$  spin-0 orbital-polarized configuration, in good agreement with experimental observations. Our proposed procedure, while straightforward to implement in standard DFT calculations, is expected to greatly facilitate a proper understanding of the dominant valance and orbital structure of strongly correlated materials at eV (or sub-eV) scale, thus setting a realistic foundation for studying even lower-energy dynamics of physical properties in functional materials.

*Quantized effective description* - As a simple illustration for such an emergent structure, consider a two-site Hubbard model,

$$H = -t \sum_{\mu} (c_{1\mu}^\dagger c_{2\mu} + c_{2\mu}^\dagger c_{1\mu}) + U(c_{1\uparrow}^\dagger c_{1\downarrow}^\dagger c_{1\downarrow} c_{1\uparrow} + c_{2\uparrow}^\dagger c_{2\downarrow}^\dagger c_{2\downarrow} c_{2\uparrow}), \quad (1)$$

containing two electrons, where  $t$  denotes the kinetic hopping between site 1 and 2,  $\mu$  the quantized spin index ( $\uparrow, \downarrow$ ), and  $U$  the charging energy when both electrons are located in the

same site. Let's first examine the emergent low-energy effective theories [31] of this system in its two representative regimes with  $t \ll U$  and  $t \gg U$ .

For  $t \ll U$ , states with doubly occupied orbitals are of high energy. Upon decoupling these states from the remaining low-energy sector via a unitary transformation of the basis [32–35] (denoting  $-\mu$  as  $\bar{\mu}$ ),

$$\begin{aligned} \tilde{c}_{i\mu}^\dagger &= \mathcal{U}^\dagger c_{i\mu}^\dagger \mathcal{U} & (2) \\ &= c_{i\mu}^\dagger + (\sin \frac{\theta}{2}) \frac{1}{2} [c_{i\mu}^\dagger (c_{i\bar{\mu}}^\dagger c_{i'\bar{\mu}} - c_{i'\bar{\mu}}^\dagger c_{i\bar{\mu}}) + c_{i'\bar{\mu}}^\dagger (n_{i'\bar{\mu}} - n_{i\bar{\mu}})] \\ &\quad + (\cos \frac{\theta}{2} - 1) \frac{1}{2} [c_{i'\bar{\mu}}^\dagger (c_{i\bar{\mu}}^\dagger c_{i'\bar{\mu}} + c_{i'\bar{\mu}}^\dagger c_{i\bar{\mu}}) + c_{i\bar{\mu}}^\dagger (n_{i\bar{\mu}} + n_{i'\bar{\mu}})], \end{aligned}$$

into the dressed particles,  $\tilde{c}_{i\mu}^\dagger$  with  $\mathcal{U} = \exp\left(\frac{\theta}{2} \sum_\mu \frac{1}{2} (c_{1\mu}^\dagger c_{2\mu} - c_{2\mu}^\dagger c_{1\mu})(n_{2\bar{\mu}} - n_{1\bar{\mu}})\right)$  and setting  $U \sin \theta - 4t \cos \theta = 0$ , the resulting effective theory for the remaining low-energy subspace (constrained by  $\tilde{c}_{1\uparrow}^\dagger \tilde{c}_{1\downarrow}^\dagger = \tilde{c}_{2\uparrow}^\dagger \tilde{c}_{2\downarrow}^\dagger = 0$ ),

$$\tilde{H}^{(t \ll U)} = \tilde{J}_{12} (\tilde{\mathbf{S}}_1 \cdot \tilde{\mathbf{S}}_2 - \frac{1}{4}), \quad (3)$$

contains one dressed particle in each site  $i = 1, 2$  interacting with each other via anti-ferromagnetic super-exchange  $\tilde{J}_{12} = \frac{U}{2} (\cos \theta - 1) + 2t \sin \theta = \frac{1}{2} (\sqrt{U^2 + (4t)^2} - U)$ , where  $\tilde{\mathbf{S}}_i = \sum_{\mu\nu} \tilde{c}_{i\mu}^\dagger \sigma_{\mu\nu} \tilde{c}_{i\nu}^\dagger$  denotes the total spin of the *dressed* particles via Pauli matrices  $\sigma_{\mu\nu}$ . Essentially, the rare occasion with bare particles temporarily double-occupying a site is *fully absorbed* into the internal structure of the dressed particles  $\tilde{c}_{i\mu}^\dagger$  such that they no longer have charge degree of freedom at longer time (lower-energy) scale.

On the other hand, in the  $t \gg U$  regime, the rapid dynamics between sites leads to formation of the bonding orbital,  $b_\mu^\dagger \equiv \frac{1}{\sqrt{2}} (c_{1\mu}^\dagger + c_{2\mu}^\dagger)$ , and the anti-bonding orbital,  $a_\mu^\dagger \equiv \frac{1}{\sqrt{2}} (c_{1\mu}^\dagger - c_{2\mu}^\dagger)$ ,

$$\begin{aligned} H &= t \sum_\mu (-b_\mu^\dagger b_\mu + a_\mu^\dagger a_\mu) & (4) \\ &\quad + \frac{U}{2} \prod_\mu (b_\mu^\dagger b_\mu + a_\mu^\dagger a_\mu) + \frac{U}{2} \prod_\mu (a_\mu^\dagger b_\mu + b_\mu^\dagger a_\mu). \end{aligned}$$

Intuitively, the state with both electrons occupying the anti-bonding orbital has a very high energy. Upon decoupling it from the lower-energy subspace via a unitary transformation  $\mathcal{V} = \exp\left(\frac{\phi}{2} (a_\uparrow^\dagger a_\downarrow^\dagger b_\uparrow^\dagger b_\downarrow - b_\uparrow^\dagger b_\downarrow^\dagger a_\uparrow a_\downarrow)\right)$  of the basis,

$$\begin{aligned} \tilde{b}_\mu^\dagger &= b_\mu^\dagger - (\sin \frac{\phi}{2}) a_\mu^\dagger a_\mu^\dagger b_{\bar{\mu}} + (\cos \frac{\phi}{2} - 1) b_\mu^\dagger b_\mu^\dagger b_{\bar{\mu}}, \\ \tilde{a}_\mu^\dagger &= a_\mu^\dagger + (\sin \frac{\phi}{2}) b_\mu^\dagger b_\mu^\dagger a_{\bar{\mu}} + (\cos \frac{\phi}{2} - 1) a_\mu^\dagger a_\mu^\dagger a_{\bar{\mu}}, \end{aligned} \quad (5)$$

and setting  $4t \sin \phi - U \cos \phi = 0$ , the resulting effective Hamiltonian for the low-energy subspace (constrained by  $\tilde{a}_\uparrow^\dagger \tilde{a}_\downarrow^\dagger = 0$ ),

$$\tilde{H}^{(t \gg U)} = \sum_\mu (\tilde{\epsilon}_b \tilde{b}_\mu^\dagger \tilde{b}_\mu + \tilde{\epsilon}_a \tilde{a}_\mu^\dagger \tilde{a}_\mu) - \tilde{J}_{ba} \tilde{\mathbf{S}}_b \cdot \tilde{\mathbf{S}}_a, \quad (6)$$

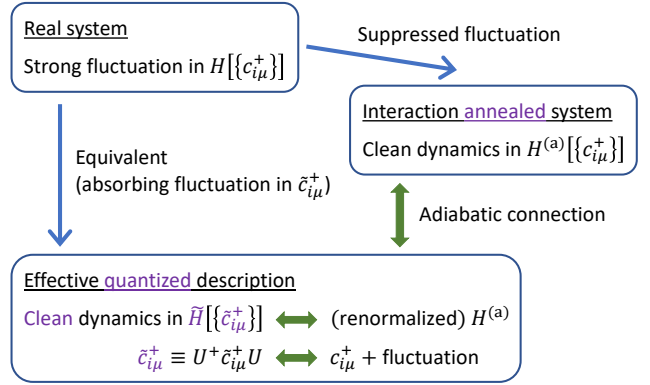


FIG. 1. Illustration on obtaining effective *quantized* description through interaction annealing procedure. Real systems  $H$  described by bare particle  $c_i^\dagger$  typically contain strong fluctuation that masks the dominant physics. Equivalently, the low-energy dynamics can always be described by some fully quantized  $\tilde{H}$  via absorbing the fluctuation into dressed particles  $\tilde{c}_i^\dagger$ . The desired effective description can be acquired through the bare description of a fictitious interaction ‘annealed’ systems,  $H^{(a)}$  with suppressed fluctuation, given the adiabatic connection between them.

has instead an emergent ferromagnetic inter-orbital Hund’s coupling of strength  $\tilde{J}_{ba} = U$  and the renormalized orbital energy  $\tilde{\epsilon}_b = -t \cos \phi + \frac{U}{4} (1 - \sin \phi) = -\frac{1}{4} (\sqrt{(4t)^2 + U^2} - U)$  and  $\tilde{\epsilon}_a = -\tilde{\epsilon}_b + \frac{\tilde{J}_{ba}}{4}$ .

One sees that in these two limits, the low-energy dynamics are described by different emergent physics. It is precisely such abundant choices of low-energy effective description that generally produces the rich complex behaviors of correlated materials [3, 8] Nonetheless, notice that in either case above, the low-energy dynamics can be *exactly* described by an effective theory containing only *quantized* charge, orbital, and spin degrees of freedom.

In fact, as illustrated in Fig. 1, generally there always exists at least one such fully quantized description upon *absorbing* the less essential fluctuations into the internal structure of dressed particles. In the intermediate  $2t/U = 1$  regime of this example, Eq. 3 remains an exact representation of the low-energy dynamics, just with a heavily renormalized parameter  $\tilde{J}_{12}$  beyond perturbation. All strong fluctuations can still be *fully absorbed* in  $\tilde{c}_{i\mu}^\dagger$  to allow a quantized description. For example the size of spin of the dressed particles  $\langle \tilde{S}^2 \rangle = \frac{3}{4}$  corresponds to a quantized spin-1/2 [36], even though expectation values of most observables of *bare* particles, e.g.  $\langle S^2 \rangle \sim 0.54 < \frac{3}{4}$ , deviate far from those of quantized values, as typically found in DFT calculations.

The above example illustrates the quantum mechanical origin of the widely applied *integer* valance count in chemistry [37]: The most essential low-energy dynamics are fully accounted for by such an emergent quantized description. Therefore, seeking a dominant quantized structure, as often exercised in chemistry, is not simply for convenience, but rather an important task fully justified by rigorous quantum many-body physics that grants direct access to the essential

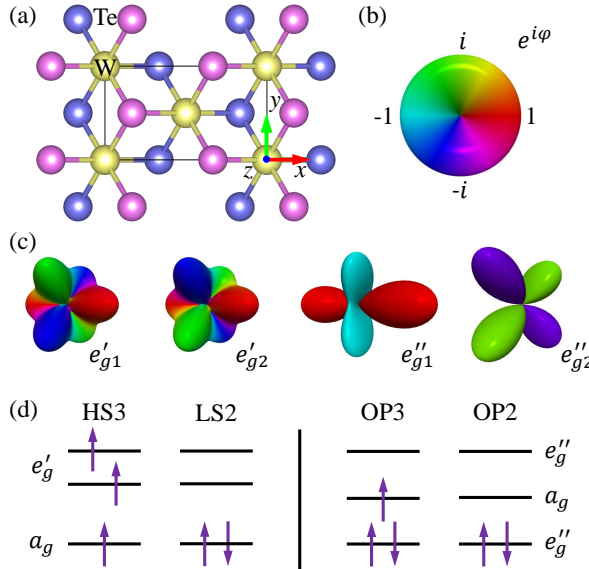


FIG. 2. (color online) (a) Top view the higher symmetry 1T lattice structure of WTe<sub>2</sub>, with W atoms in yellow and Te atoms above/below the W layer in pink/purple, showing also the local coordinate axis of W orbitals. (b) Color scheme labeling the phase of orbitals. (c) Symmetry related  $e'_g$  orbitals of W, and their symmetric superposition,  $|e''_{g1}\rangle = \frac{1}{\sqrt{2}}(|e'_{g1}\rangle + |e'_{g2}\rangle)$  and  $|e''_{g2}\rangle = \frac{1}{\sqrt{2}}(|e'_{g1}\rangle - |e'_{g2}\rangle)$  emerged in orbital polarized states [39]. (d) Potential local electronic structures, including high-spin (HS), low-spin (LS), and orbital-polarized (OP) configurations containing 2 or 3 electrons.

low-energy dynamics of the system [38]. The question is then how to obtain such a useful and powerful picture of quantized valence, orbital, and spin structure within the standard DFT calculations, especially for correlated materials displaying rich physical properties due to strong intra-atomic interactions.

*Adiabatic connection* - The answer lies in the adiabatic connection sketched in Fig. 1 between the effective quantized description of the real system and the bare description of a fictitious system with suppressed fluctuation through the artificial enhancement of the dominant physics. Using the above example as an illustration, when represented via the dressed particles, the low-energy dynamics of the realistic Hamiltonian  $\tilde{H}$ , say at  $2t/U \sim 1$ , has identical form of  $H^{(t \ll U)}$  in Eq. 3, just with a renormalized parameter  $\tilde{J}_{12}$ . Therefore,  $\tilde{c}_i^\dagger$  of the realistic  $H$  can literally be viewed as the bare particle  $c_i^\dagger$  of  $H$  with additional fluctuation absorbed inside  $\tilde{c}_i^\dagger$ , as shown in Eq. 2.

In other words, by suppressing the fluctuation through artificially enhancing the dominant interaction  $U$ , the resulting bare particles  $c_{i\mu}^\dagger$  actually adiabatically connect to the dressed particles  $\tilde{c}^\dagger$  with qualitatively the same low-energy dynamics. In realistic materials, this general property of many-body Hamiltonian should apply to systems with open  $d$ - and  $f$ -shells containing strong intra-atomic interactions. Below we proceed to demonstrate such adiabatic connection in real materials within an affordable LDA+ $U$  approaches [40, 41] that

TABLE I. One-body density matrix  $\rho_{nn'}$  among the local W  $t_{2g}$  orbitals with index  $n$ . For a realistic strength of intra-atomic interaction  $U \sim 3$  eV, the upper part of the table shows fractional occupation in all three orbitals (c.f. the diagonal elements) due to strong quantum charge fluctuation. The lower part gives the  $\rho_{nn'}$  for OP2(FO2) at high- $U$ , one of the three survived OP2 configurations. Upon diagonalizing  $\rho_{nn'}$ , this configuration contains only one occupied orbital  $e''_{g2}$ . Both cases shown here have identical  $\rho_{nn'}$  for the up- and down-spin channels.

$\rho_{nn'}$	$a_g$	$e'_{g1}$	$e'_{g2}$
$U \sim 3$ eV	0.32	0.00	0.00
	0.00	0.35	0.00
	0.00	0.00	0.35
$U \sim 20$ eV	0.06	0.02	0.02
	0.02	0.45	-0.36
	0.02	-0.36	0.45
$\rho_{nn'}$	$a_g$	$e''_{g1}$	$e''_{g2}$
$U \sim 20$ eV	0.06	0.02	0.02
	0.02	0.09	0
	0.02	0	0.81

employs an effective Hartree-Fock treatment [42]. (This implementation [40] accounts for the effective self-interaction such that the energetic sequence relative to the ligand orbitals is retained upon suppressing charge fluctuations via enlarged  $U$ .)

As a generic example, consider the semi-metallic material WTe<sub>2</sub> [17, 18] that contains W atoms with open  $d$ -shell surrounded by edge-sharing octahedra of Te atoms, as shown in Fig. 2. The standard LDA+ $U$  calculation with a reasonable value of  $U = 3$  eV [43] gives a highly fluctuating one-body density matrix (c.f. Tab I) that is difficult to map to a purely quantized valence and orbital structure desired for physical understanding as discussed above. In great contrast, if one artificially ‘heats up’ the intra-atomic interaction  $U$  of the system to a large value, say 20 eV, one would suppress the quantum charge fluctuation and find a much better-defined valence, orbital, and spin structure, for example, the one shown in the lower part of Tab. I.

In order to also reveal the potential spontaneous symmetry breaking of the system, this demonstration employs the idealized 1T structure of higher symmetry shown in Fig. 2(a), instead of the experimental structure that biases a particular broken symmetry. Once the dominant electronic structure with a particular broken symmetry is identified, further structural relaxation would result in a lattice structure with corresponding lower symmetry.

In fact, at this high- $U$  regime, one finds many stable structures, as shown in Fig. 2(d), all with distinct well-defined ionic valence, orbital, and spin structures. Among the original  $t_{2g}$  complex, these include a  $d^3$  high-spin (HS3), a  $d^2$  low-spin (LS2), a  $d^3$  orbital polarized low-spin (OP3), and a  $d^2$  orbital polarized low-spin (OP2) configurations. One can even stabilize states containing different spatial ordering of these

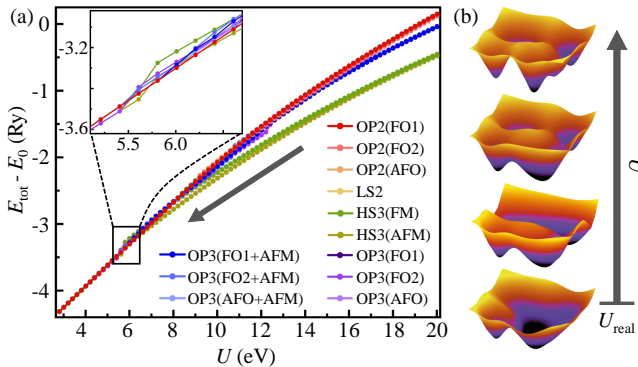


FIG. 3. (color online) Demonstration of the adiabatic connection between ‘clean’ high- $U$  configurations and the strongly fluctuating ones with realistic  $U$ , through a smooth evolution of total energy upon reduction of  $U$ . Here the total energy is for 4 chemical formula units and presented relative to a reference  $E_0$ . (a) Starting from stable LDA+ $U$  solution of WTe<sub>2</sub> at high- $U$ , with slowly increased fluctuation via reduction of  $U$ , configurations typically evolve smoothly, unless the corresponding configurations become unstable at lower  $U$  and fall into another stable configuration, as emphasized in the inset. (b) Destabilization of these configurations corresponds to the removal of energy local minima upon lowering of the energy barriers between them. Stable ionic configurations [c.f. Fig. 2(d)] can further develop ferro-orbital (FO), anti-ferro-orbital (AFO), ferromagnetic (FM), and antiferromagnetic (AFM) long-range orders.

ionic structures, such as ferro-orbital order (FO), antiferro-orbital order (AFO), ferromagnetic order (FM), and antiferromagnetic order (AFM). Each of these stable structures corresponds to distinct low-energy dynamics that give rise to a variety of physical properties. Such abundant choices of stable structures are precisely why correlated materials display rich functionalities suitable for various applications.

Figure 3(a) demonstrates the above-mentioned adiabatic connection between the artificially high- $U$  structures and the realistic system under a fixed set of external parameters, such as pressure, temperature, and external fields (in this case the fixed lattice structure). As the value of  $U$  slowly ‘cools down’, the growing quantum fluctuation can conceptually be *fully* absorbed into the *dressed*  $\tilde{e}_g'$  orbitals, such that the fully quantized description is maintained and correspondingly the total energies smoothly evolve as well.

Physically, one does not expect all of these high- $U$  structures to remain stable at lower- $U$  regime for a fixed external condition. Indeed, in Fig. 3(a) some of the structures fall to another more stable configuration with the obvious change in the total energy and the one-body density matrix, as emphasized in the inset. In this particular case, by  $U < 5$  eV only OP2 and LS2 configurations survive, and the former has the lowest energy since  $U < 12$  eV. This indicates that in real material the electronic correlation at the Rydberg scale already produces a tendency toward a local orbital polarization and at a lower energy scale a long-range ferro-orbital ordering. The experimentally observed  $T_d$  structure is therefore driven by such electronic correlation, assisted by further energy gain upon corresponding lattice relaxation.

Figure 3(b) illustrates the microscopic mechanism for such

destabilization of some of the high- $U$  configurations, via the energy contour as a function of the one-body density matrix. As one ‘cools down’  $U$ , the energy contour continuously deformed. Upon removal of the barriers between the local minima, the locally stable configurations at high- $U$  would then drop to the more stable configurations, producing the transition behavior shown in the inset of Fig. 3(a). Of course, under different external conditions, the deformation can vary and result in qualitatively distinct low- $U$  configurations and their associated physical properties. Nonetheless, one sees that the most important ground state at the realistic value of  $U$  is always adiabatically connected to one high- $U$  electronic structure that has a well-defined valence, orbital, and spin structure.

*‘Interaction annealing’ procedure* - The adiabatic connection demonstrated above therefore indicates a simple yet generic computational ‘interaction annealing’ procedure to decipher the dominant effective local electronic structure that controls the low-energy dynamics in correlated materials. Given that one of the stable electronic structures at large  $U$  is adiabatically connected to the realistic system, one can therefore slowly ‘heat up’ the interaction strength of the realistic system, until the corresponding one-body density matrix displays a clear quantization of valence, orbital, and spin for an unambiguous identification of the dominant effective emergent picture.

Specific for WTe<sub>2</sub>, the ground state with the experimentally observed  $T_d$  structure under a realistic value of  $U$  contains a heavily mixed local density matrix  $\rho_{nn'}$  of orbital  $n$  nearly identical [31] to the upper part of Tab. I. This reflects strong fluctuations of the  $t_{2g}$  subspace of the 5d orbitals in real materials that mask the essential quantized structure for the low-energy dynamics. Upon steadily suppressing the fluctuation via slowing ‘heating up’  $U$  to 20 eV, one finds a cleaner  $\rho_{nn'}$  as in Tab. I. In the rotated basis,  $e_g''$  [c.f. Fig. 2(c)]  $\rho_{nn'}$  gives a well-defined valence, orbital, and spin structure as in the lower part of Tab. I, corresponding to a quantized *emergent* OP2 structure shown in Fig. 2(d). One thus can reliably describe the electronic structure and its dynamics of the real material via an effective OP2 structure with dressed particles in  $\tilde{e}_g''$  orbitals that absorb the less essential fluctuations.

Specifically, the energetically most stable OP2(FO2) configuration contains W ions with double occupation of one of the symmetry-related dressed  $\tilde{e}_g''$  orbitals, as adiabatically connected to the one-body density matrix of a high- $U$  configuration shown in the lower part of Tab. I. In the absence of long-range order, there would be another symmetry-related configuration with both electrons occupying the other dressed  $\tilde{e}_g''$  orbitals. Correspondingly, the low-energy dynamics must then contain that of an effective pseudo-spin-1/2 orbital fluctuation, or ‘orbiton’. In great contrast, such an understanding is not possible from the heavily fluctuating density matrix of the bare  $e_g'$  orbitals as in Tab. I.

Furthermore, our OP2(FO2) configuration gives a *ferro-orbital ordering* of the dressed  $\tilde{e}_g''$  orbitals of W. The high-energy (Rydberg) scale of the driving force for such a ferro-orbital order thus offers a natural explanation for the exper-

TABLE II. Estimated octahedral distortion from ionic radius [46] for  $d^2$  and  $d^3$  configurations in WTe<sub>2</sub> with  $T_d$  structure, in comparison with the experimental parameter. Distortion is evaluated by the shortest W-Te bond length,  $\Delta = \sum_{i=1}^6 |d_i - d_{\text{mean}}|$ , and distortion parameters,  $\Sigma = \sum_{i=1}^{12} |90 - \phi_i|$ , where  $\phi_i$  denotes the intersection angle  $B_{i_1} - A - B_{i_2}$  of octahedron  $AB_6$ .

$T_d$ structure	$d^2$	$d^3$
experiment [44]	configuration	configuration
$\Delta(\text{\AA})$	0.306	0.073
$\Sigma(^{\circ})$	145.200	162.963
		204.611

imentally observed deformation of  $T_d$  lattice structure of this material below  $\sim 550\text{K}$  of temperature [44] and 6 GPa of pressure [45], since the lattice couples to the electronic charge and would therefore follow the electronic ordering.

Indeed, as shown in Tab. II, the experimental observation of octahedral lattice distortion agrees much better with simple estimation using ionic radius of  $d^2$  W ion than that via  $d^3$  W ion [46]. Similarly, the spin-0 structure of OP2 agrees perfectly with the experimental observation of a diamagnetic response in WTe<sub>2</sub> [47]. These agreements with experiments confirm that the ferro-orbital ordered spin-0 picture obtained from the above adiabatic connection indeed captures the dominant short-range higher-energy correlation of WTe<sub>2</sub>. One thus can start from this realistic structure of intermediate energy scale to investigate further lower-energy-scale physics, such as the observed weak ferroelectricity [22, 23, 48] and transport properties [20, 28–30], via methods suitable for longer-range correlation.

In summary, we propose a simple yet generic ‘interaction annealing’ approach of density functional calculations to gain access to the local electronic structure that dominates the low-energy dynamics of correlated materials. Using a simple two-site Hubbard model and ferroelectric WTe<sub>2</sub> as representative examples, we first illustrate the *rigorous* existence of effective descriptions containing fully quantized structures. We then demonstrate their adiabatic connection to those with suppressed charge fluctuation. This in turn leads to our proposal of ‘interaction annealing’ procedure to identify the dominant quantized structure by slowly ‘heating up’ the interaction within LDA+ $U$  approach of DFT. Specifically for WTe<sub>2</sub>, this analysis indicates a  $d^2$  spin-0 configuration containing a ferro-orbital order of dressed  $\tilde{e}_g''$  orbitals that produce the experimentally observed diamagnetism and lower-symmetry lattice structure. Applications of the proposed simple procedure and the resulting effective physical picture are expected to greatly facilitate a proper understanding of local dynamics in a wide range of correlated materials.

We acknowledge helpful discussions with Zhiyu Fan. This work is supported by the National Natural Science Foundation of China (NSFC) under Grants No. 12274287 and No. 12042507 and the Innovation Program for Quantum Science and Technology No. 2021ZD0301900.

\* These authors contributed equally.

† corresponding email: weiku@sjtu.edu.cn

- [1] in *The Coming of Materials Science*, Pergamon Materials Series, Vol. 5, edited by R. W. Cahn (Pergamon, 2001) pp. 253–304.
- [2] D. Sahu, *Functional Materials* (IntechOpen, Rijeka, 2019).
- [3] E. Dagotto, *Science* **309**, 257 (2005).
- [4] M. Kawai, F. Nabeshima, and A. Maeda, *Journal of Physics: Conference Series* **1054**, 012023 (2018).
- [5] Y. S. Kushnirenko, A. A. Kordyuk, A. V. Fedorov, E. Haubold, T. Wolf, B. Büchner, and S. V. Borisenko, *Phys. Rev. B* **96**, 100504(R) (2017).
- [6] H. Sun, M. Huo, X. Hu, J. Li, Y. Han, L. Tang, Z. Mao, P. Yang, B. Wang, J. Cheng, D.-X. Yao, G.-M. Zhang, and M. Wang, *Nature* **493** (2023).
- [7] Y. Cao, V. Fatemi, S. Fang, K. Watanabe, T. Taniguchi, E. Kaxiras, and P. Jarillo-Herrero, *Nature* **556**, 43 (2018).
- [8] P. W. Anderson, *Science* **177**, 393 (1972).
- [9] L. Bellaiche and D. Vanderbilt, *Physical Review Letters* **81**, 1318 (1998).
- [10] Z. Wu and H. Krakauer, in *Fundamental Physics of Ferroelectrics 2000: Aspen Center for Physics Winter Workshop*, American Institute of Physics Conference Series, Vol. 535 (2000) pp. 121–128.
- [11] V. Stevanović, M. d’Avezac, and A. Zunger, *Phys. Rev. Lett.* **105**, 075501 (2010).
- [12] V. Stevanović, M. d’Avezac, and A. Zunger, *Journal of the American Chemical Society* **133**, 11649 (2011), pMID: 21702454, <https://doi.org/10.1021/ja2034602>.
- [13] P. Hohenberg and W. Kohn, *Phys. Rev.* **136**, B864 (1964).
- [14] W. Kohn and L. J. Sham, *Phys. Rev.* **140**, A1133 (1965).
- [15] J. Hubbard, *Proceedings of the Royal Society of London. Series A, Mathematical and Physical Sciences* **276**, 238 (1963).
- [16] D. P. Arovas, E. Berg, S. A. Kivelson, and S. Raghu, *Annual Review of Condensed Matter Physics* **13**, 239 (2022).
- [17] C.-H. Lee, E. C. Silva, L. Calderin, M. A. T. Nguyen, M. J. Hollander, B. Bersch, T. E. Mallouk, and J. A. Robinson, *Scientific Reports* **5**, 10013 (2015).
- [18] P. K. Das, D. D. Sante, F. Cilento, C. Bigi, D. Kopic, D. Sorianzio, A. Sterzi, J. A. Krieger, I. Vobornik, J. Fujii, T. Okuda, V. N. Strocov, M. B. H. Breese, F. Parmigiani, G. Rossi, S. Piccozzi, R. Thomale, G. Sangiovanni, R. J. Cava, and G. Panaccione, *Electronic Structure* **1**, 014003 (2019).
- [19] X. Qian, J. Liu, L. Fu, and J. Li, *Science* **346**, 1344 (2014).
- [20] M. Ali, J. Xiong, S. Flynn, J. Tao, Q. Gibson, L. Schoop, T. Liang, N. Haldolaarachchige, M. Hirschberger, N. Ong, and R. Cava, *Nature* **514**, 205 (2014).
- [21] A. Singh, S. Sasmal, K. K. Iyer, A. Thamizhavel, and K. Maiti, *Phys. Rev. Mater.* **6**, 124202 (2022).
- [22] Z. Fei, W. Zhao, T. Palomaki, B. Sun, M. Miller, Z. Zhao, J.-Q. Yan, X. Xu, and D. Cobden, *Nature* **560** (2018), 10.1038/s41586-018-0336-3.
- [23] P. Sharma, F.-X. Xiang, D.-F. Shao, D. Zhang, E. Y. Tsymbal, A. R. Hamilton, and J. Seidel, *Science Advances* **5**, eaax5080 (2019).
- [24] X. Pan, Y. Pan, J. Jiang, H. Zuo, H. Liu, X. Chen, Z. Wei, S. Zhang, Z. Wang, X. Wan, Z. Yang, D. Feng, Z. Xia, L. Li, F. Song, B. Wang, Y. heng Zhang, and G. Wang, *Frontiers of Physics* **12**, 127203 (2017).
- [25] L. R. Thoutam, Y. L. Wang, Z. L. Xiao, S. Das, A. Luican-Mayer, R. Divan, G. W. Crabtree, and W. K. Kwok, *Phys. Rev.*

Lett. **115**, 046602 (2015).

[26] D. Khomskii, K. Kugel, A. Sboychakov, and S. Streltsov, *Journal of Experimental and Theoretical Physics* **122** (2015), 10.1134/S1063776116030079.

[27] S. Ji, O. Granas, and J. Weissenrieder, *ACS Nano* **15**, 8826 (2021), pMID: 33913693, <https://doi.org/10.1021/acsnano.1c01301>.

[28] A. A. Soluyanov, D. Gresch, Z. Wang, Q. Wu, M. Troyer, X. Dai, and B. A. Bernevig, *Nature* **527**, 495 (2015).

[29] Q. Ma, S.-Y. Xu, H. Shen, D. MacNeill, V. Fatemi, T.-R. Chang, A. M. Mier Valdivia, S. Wu, Z. Du, C.-H. Hsu, S. Fang, Q. D. Gibson, K. Watanabe, T. Taniguchi, R. J. Cava, E. Kaxiras, H.-Z. Lu, H. Lin, L. Fu, N. Gedik, and P. Jarillo-Herrero, *Nature* **565**, 337 (2019).

[30] H. Wang and X. Qian, *npj Computational Materials* **5**, 119 (2019).

[31] See supplementary for details.

[32] K. Chao, J. Spalek, and A. Oles, *Journal of Physics C: Solid State Physics* **10**, L271 (1977).

[33] S. White, *The Journal of Chemical Physics* **117** (2002), 10.1063/1.1508370.

[34] J. Feist and contributors, “Quantumalgebra.jl,” (2021).

[35] M. Sánchez-Barquilla, R. E. F. Silva, and J. Feist, *J. Chem. Phys.* **152**, 034108 (2020).

[36] J. J. Sakurai, *Modern quantum mechanics; rev. ed.* (Addison-Wesley, Reading, MA, 1994).

[37] Ruoshi Jiang, Xiang Li, Xinyao Zhang and Wei Ku, in preparation.

[38] R. Jiang, J. Hou, Z. Fan, Z.-J. Lang, and W. Ku, *Phys. Rev. Lett.* **132**, 126503 (2024).

[39] Z. Qian and G. Khaldoon, “Spherical harmonics visualization,” (2013).

[40] V. I. Anisimov, I. V. Solovyev, M. A. Korotin, M. T. Czyzyk, and G. A. Sawatzky, *Phys. Rev. B* **48**, 16929 (1993).

[41] A. I. Liechtenstein, V. I. Anisimov, and J. Zaanen, *Phys. Rev. B* **52**, R5467 (1995).

[42] V. I. Anisimov, F. Aryasetiawan, and A. I. Lichtenstein, *Journal of Physics: Condensed Matter* **9**, 767 (1997).

[43] N. E. Kirchner-Hall, W. Zhao, Y. Xiong, I. Timrov, and I. Dabo, *Applied Sciences* **11** (2021), 10.3390/app11052395.

[44] Y. Tao, J. A. Schneeloch, A. A. Aczel, and D. Louca, *Phys. Rev. B* **102**, 060103 (2020).

[45] Y. Zhou, X. Chen, N. Li, R. Zhang, X. Wang, C. An, Y. Zhou, X. Pan, F. Song, B. Wang, W. Yang, Z. Yang, and Y. Zhang, *AIP Advances* **6**, 075008 (2016).

[46] R. D. Shannon, *Acta crystallographica section A: crystal physics, diffraction, theoretical and general crystallography* **32**, 751 (1976).

[47] L. Yang, H. Wu, L. Zhang, W. Zhang, L. Li, T. Kawakami, K. Sugawara, T. Sato, G. Zhang, P. Gao, Y. Muhammad, X. Wen, B. Tao, F. Guo, and H. Chang, *Advanced Functional Materials* **31**, 2008116 (2021).

[48] Fangyuan, Ruoshi Jiang and Wei Ku, in preparation.